p-d scattering with a nonlocal nucleon-nucleon potential below the breakup threshold

P. Doleschall*
Research Institute for Particle and Nuclear Physics, Budapest, Hungary

Z. Papp
Department of Physics and Astronomy, California State University, Long Beach, 90840 California and Institute of Nuclear Research of the Hungarian Academy of Sciences, Debrecen, Hungary

(Received 31 May 2005; published 26 October 2005)

A short-range nonlocal nucleon-nucleon potential, which previously provided a better description for the three-nucleon bound states ^3H and ^{3}He then the local-potential models, is tested in *p-d* scattering calculations at energies below the three-body breakup threshold. This potential again provides an equivalent or better description of the experimental data than the local Argonne+3N force model.

DOI: 10.1103/PhysRevC.72.044003 PACS number(s): 21.30.−x, 21.45.+v, 21.10.Dr, 25.40.−h

I. INTRODUCTION

Recently, in a series of articles, a nonlocal nucleon-nucleon (NN) interaction has been proposed [1,2]. The potential is nonlocal inside and Yukawa-type outside (INOY = inside nonlocal and outside Yukawa) and the nonlocality is of shorter range than in the earlier nonlocal models [3,4]. The local Yukawa tail was cut off in the region from 1 to 3 fm, i.e., below 1 fm there is no local potential at all, whereas around 3 fm the local potential becomes the intact Yukawa tail. The internal nonlocal potential was subsequently fitted to the NN data, whereas the local potential was kept fixed. The overlap region of the local and the fitted nonlocal interactions is practically the same interval from 1 to 3 fm as the cutoff region of the Yukawa tail, although the nonlocal interaction is rather small outside 2–2.5 fm. Its bulk is within the 1.5-fm sphere, which is in accordance with the more rigorous expectation on the range of the nonlocality [5].

This new shorter range IS (INOY with Short range nonlocality) potential includes the charge independence and charge symmetry breaking effects in the $^1S_0$ component. The *nn*, *pp*, and *np* interactions are slightly different and fit perfectly the *pp* and *np* data and the *nn* scattering length [1,2]. The higher partial-wave components of the nonlocal interaction have no charge symmetry breaking effect; the nuclear part of the *nn* and *pp* interactions is the same.

All interactions were calculated with equal neutron and proton masses and without electromagnetic terms, and only the nonrelativistic Coulomb interaction was taken into account for the *pp* pair with a charge distribution defined in Ref. [6]. This approximation (equal neutron and proton masses, the lack of the electromagnetic corrections, and the nonrelativistic Coulomb interaction) slightly changes the deuteron binding energy and the zero energy observables produced by the original Argonne v_{18} potential [7]. Therefore a small correction to the nuclear part of the original Argonne v_{18} potential is added to reproduce the correct scattering lengths and deuteron binding energy. This modified Argonne potential, denoted by ARGm, produces the same $3N$ binding energies [1] than the original Argonne one (accuracy within 1–2 keV). Because both the INOY and the Argonne potentials, the original and the modified ones, have the same long range tail, the modified Argonne potential (ARGm) can be used as a reference local potential to investigate the effects of nonlocality in the INOY potential.

The IS interactions reproduce simultaneously the ^3H and ^{3}He binding energies with high accuracy [1]. This seems to be a beneficial effect of the low deuteron *D*-state probability ($P_D = 3.60\%$) and the proper tuning of the $^1S_0$ interactions. The IS $^1S_0$ and $^3SD_1$ interactions of the Ref. [1] are phenomenological model NN interactions, which do not seem to contradict the physical expectations about the nature of the NN interaction and reproduce the NN measurements with high accuracy.

This INOY-type nonlocality has been added also to the *P*- and *D*-wave channels, including the $^3PF_2$ and $^3DG_3$ channels [2]. The triplet *P*-wave INOY interactions were fitted to the slightly modified phase shifts [8] to produce better nucleon and deuteron vector analyzing powers of the *N-d* elastic scattering [2]. These *P*- and *D*-wave INOY interactions does not change the earlier achieved correct reproduction of the ^3H and ^{3}He binding energies. For the higher partial-wave components of the NN interactions the slightly modified Argonne v_{18} (ARGm) interactions are used.

In Ref. [2] the estimated Coulomb effect for the INOY interaction was deduced by comparing the *n-d* and *p-d* results of Ref. [9]. It was found that the expected Coulomb effect in most cases, and especially the characteristic minimum of the T_{22}, would improve the agreements with the experimental data.

The aim of this work is to compare the high-precision *p-d* measurements with exact *p-d* calculations and to investigate the Coulomb effects in case of the INOY interactions. For this purpose, the three-body Faddeev equations with Coulomb potential were solved by using the method of Ref. [10]. The method is sketched briefly in Sec. II, the details of the calculations are shown in Sec. III, and the evaluation of the results are in Sec. IV.

*E-mail address: doles@rmki.kfki.hu

 ©2005 The American Physical Society

II. TREATMENT OF THE COULOMB INTERACTION IN NUCLEAR THREE-BODY SYSTEMS

The three-body Hamiltonian is given by the following:

$$H = H_0 + \sum_{i=1}^{3} V_i^C + \sum_{i=1}^{3} V_i^n, \tag{1}$$

where H_0 is the kinetic energy operator and V_i^C and V_i^n, respectively, are the long-range Coulomb and the short-range nuclear interactions between the particles $j \neq i$ and $k \neq i$.

The Faddeev decomposition of the wave function

$$\Psi = \sum_{i=1}^{3} \Psi_i$$

leads to a system of equations

$$(E - H_0 - V^C - V_i^n)\Psi_i = V_i^n(\Psi_j + \Psi_k), \tag{2}$$

where $V^C = \sum_{i=1}^{3} V_i^C$ and (i, j, k) is a cyclic permutation of Eqs. (1), (2), and (3).

Introducing the channel Coulomb interactions

$$U_i^{\rm ch} = Z_i(Z_j + Z_k)/R_i,$$

where Z_i is the charge of the i-th particle and R_i is the distance between the i-th particle relative to the center of mass of the other two particles (j-th and k-th), the Eq. (2) formally could be rearranged

$$\Psi_i = \Phi_i + G_i^{\rm ch}(E)[U_i^p\Psi_i + V_i^n(\Psi_j + \Psi_k)], \tag{3}$$

where $G_i^{\rm ch}(E) = (E - H_0 - U_i^{\rm ch} - V_i^C - V_i^n)^{-1}$, $U_i^p = V_j^C + V_k^C - U_i^{\rm ch}$ is the polarization potential and Φ_i is the incoming wave function (on-shell channel distorted Coulomb wave function multiplied by the incoming two-body bound-state wave function).

This equation is solved by using the Coulomb-Sturmian expansion method of Ref. [10], which transforms the integral equation to a matrix equation. Then, the Coulomb-distorted T-matrix elements are obtained as the matrix elements of the nuclear potentials between the corresponding wave-function components. The matrix equation [Eq. (3)] can also be recast into a matrix equation for the on-shell matrix elements of the Coulomb-distorted transition operator U

$$U_{ij} = K_{ij} + \sum_{k=1}^{3} K_{ik}G_k^{\rm ch}(E)U_{kj}, \tag{4}$$

where $K_{ij} = \delta_{ij}U_i^p + (1 - \delta_{ij})V_j^n$. The operator form of this later equation has been discussed in Ref. [11].

Both matrix equations [Eqs. (3) and (4)] were iterated and solved by the Padé method [12]. It was found that 20–30 iterations are sufficient to have a convergence with the Padé technique.

III. RESULTS

The p-d calculations were performed by using the modified Argonne v_{18} (ARGm) [1] and the INOY potentials with modified triplet P-wave components (IS-M) [2]. The interactions were taken into account up to the $j_{\max} = 4$ components and Coulomb-Sturmian states up to $N = 30$–40. The results are well converged and, as far as the measurable quantities are concerned, the accuracy is better than 1%.

TABLE I. $J = 1/2^+$ and $J = 1/2^-$ K-matrix results for p-d scattering at $E_{\rm lab} = 2$ MeV with the Argonne (Ref. [13]) and the modified Argonne potentials (this work).

$E_{\rm lab}$		K_{11}	K_{12}	K_{21}	K_{22}
		$\langle J = 1/2^+ \rangle$			
1.0	Ref. [13]	−0.231	−0.0039	−0.0040	−0.0137
1.0	This work	−0.233	0.0039	0.0040	−0.0137
3.0	Ref. [13]	−0.623	−0.0107	−0.0109	−0.0629
3.0	This work	−0.626	0.0107	0.0108	−0.0629
		$\langle J = 1/2^- \rangle$			
1.0	Ref. [13]	0.145	−0.0605	−0.0606	−0.0406
1.0	This work	0.145	−0.0605	−0.0606	−0.0404

In case of n-d scattering, with a restricted set of interactions ($j_{\max} = 3$), the solution of the present techniques and the one based on separable approximation of the two-nucleon T-matrices [2] was compared and perfect agreement have been found. Because the full calculation [$j_{\max} = 4$] using the present technique is rather time consuming, the full n-d calculations [IS-M(nd)] were performed with the separable T-matrix approximation [2]. Their accuracy for the measurable quantities is also within 1%.

The numerical procedure were cross checked by using the corresponding K-matrix of the p-d scattering results of the Ref. [13]. Tables I and II show that the K-matrix elements are in good agreement, although the Argonne interaction in the present work is slightly different. The phase-factor difference $i^{l_i - l_j}$, where l_i and l_j are the angular momenta for the incoming and outgoing channels, respectively, is certainly related to the different definition of the bipolar basis. Of course, K-matrix ought to be symmetric, which may be violated by the applied numerical procedure. This approximate symmetry itself is a measure of the accuracy.

The channels up to $j_{\max} = 4$ contain the dominant part of the nuclear interaction. Although inclusion of higher partial-wave components may alter some fine details (see Ref. [13]), these changes are within the numerical accuracy

TABLE II. $J = 5/2^+$ K-matrix results for p-d scattering at $E_{\rm lab} = 2$ MeV with the Argonne (Ref. [13]) and the modified Argonne potentials (this work).

Ref. [13]	This work	Ref. [13]	This work	Ref. [13]	This work
K_{11}		K_{22}		K_{33}	
−0.0084	−0.0084	−0.0138	−0.0137	−0.0014	−0.0013
K_{12}		K_{13}		K_{23}	
0.034	0.034	−0.00072	0.00071	−0.00015	0.00015
K_{21}		K_{31}		K_{32}	
0.034	0.034	−0.00074	0.00075	−0.00015	0.00016

of this work. The calculations were performed with total angular momentum up to $J = 13/2^-$, and only components with $l \leqslant 5$ were incorporated. Calculations that do not include the $J = 11/2^-$ and $J = 13/2^-$ components and only where the $l \leqslant 4$ components were used produce practically the same results for the measurable quantities at 1 MeV; however, at 3 MeV, there are some small differences (the largest relative deviation is about 3%).

A. The differential cross sections

There are accurate low-energy measurements for the *p-d* differential cross sections [14–16]. The results of this calculations are shown in Figs. 1–6. All the used potentials provide a good overall description of the data; the cross sections are sensitive to the fine details of the potentials only around the minima. These angle regions are shown in separate figures.

Around the minima, the experimental data are excellently reproduced by the IS-M set of interactions and the Argonne v_{18} plus the Urbana 3N force (ARG+UR) (calculations by Kievsky *et al*. [14]), whereas the results of ARGm are off. This success is because of the fact that the minimum of the differential cross section at low energy is strongly influenced by the $J = 1/2^+$ channel [17], which is also related to the ^{3}He binding energy. This binding energy is well reproduced by both the IS-M and the ARG+UR forces. Therefore the result of Ref. [14] is not a new "evidence for the three nucleon force," but just the same effect what a properly normalized 3N force produces for the 3N binding energies.

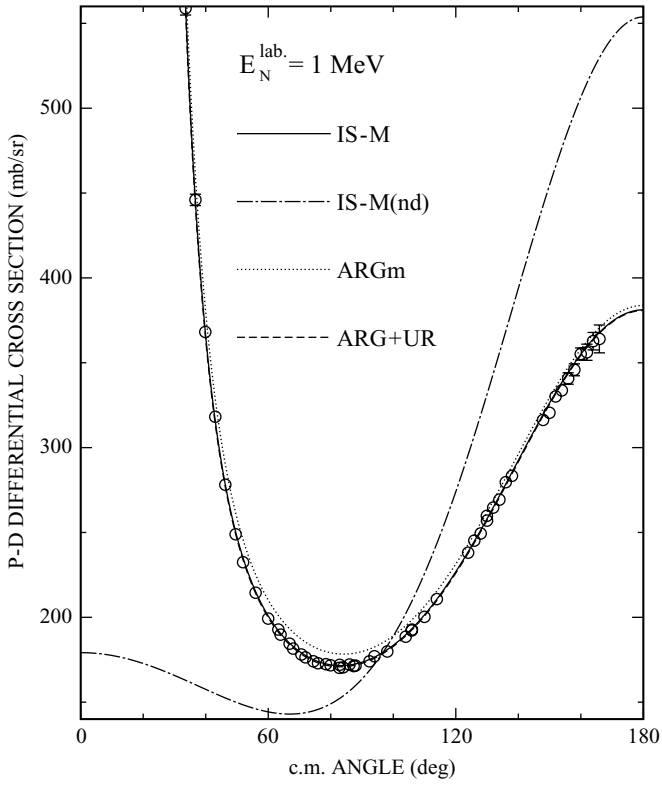

FIG. 1. *p-d* differential cross sections at a laboratory energy of 1 MeV. The experimental points are the measurement of Wood *et al*. [14].

B. The vector-analyzing powers

The theoretical description of the vector-analyzing powers up to 30 MeV is rather problematic. Their dominant dependence on the NN triplet *P*-wave interactions is well known [18,19]. By changing the triplet *P*-wave interactions one may improve the theoretical description [2]. However, the agreement between the theory and experiments are not fully satisfactory yet. The same could be said about the present results, which are shown in Figs. 7–12.

Although the calculated deuteron vector-analyzing powers are reasonable at all the three energies, the calculated proton-analyzing powers are somewhat smaller and at 1 MeV the calculated maximum is significantly lower than the measured one (Fig. 7).

C. The tensor-analyzing powers

The *p-d* tensor-analyzing power experimental results are available at 1 MeV [20] and 3 MeV [15] energies. The present calculations are shown in Figs. 13–18. The Coulomb effect is sizable and the IS-M results, in all cases, are better or equivalent with those of the ARGm or ARG+UR interaction. The Coulomb effect predicted before in Ref. [2] is proved to be correct: the changes due to the Coulomb interaction are similar to those observed at higher energies.

The most remarkable is the agreement between the IS-M results and the experiments for the T_{22} at the backward angle minimum. Although the 1-MeV measurements are not accurate enough, at 3 MeV the error bars of the experimental

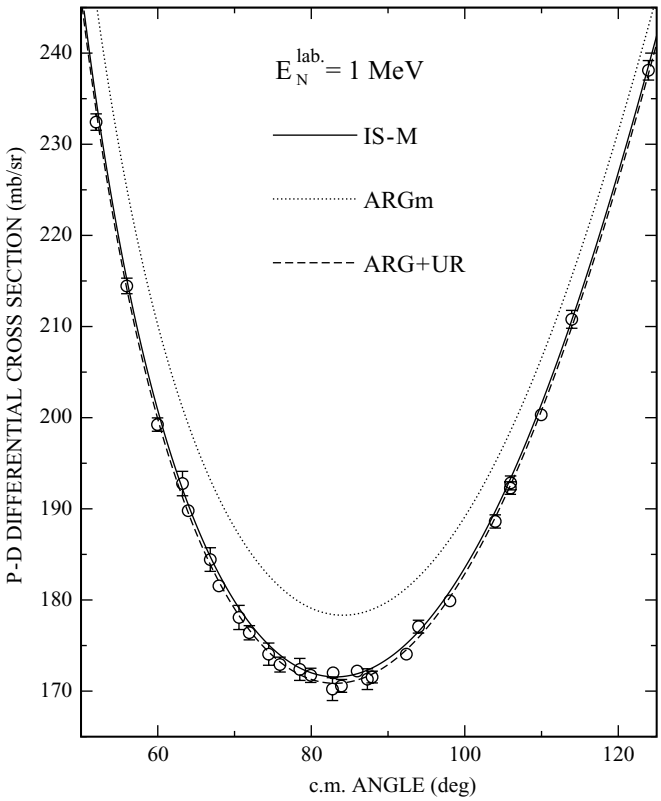

FIG. 2. The same as in Fig. 1 around the minimum region.

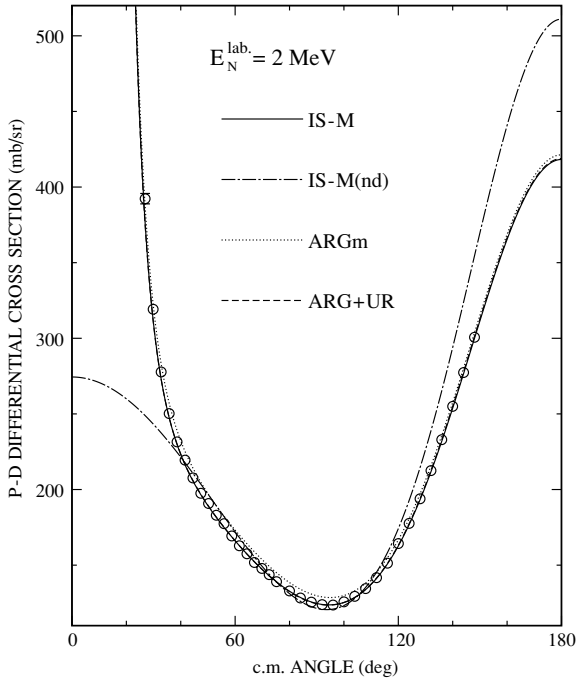

FIG. 3. *p-d* differential cross sections at a laboratory energy of 2 MeV. The experimental points are the measurement of Shimizu *et al*. [15].

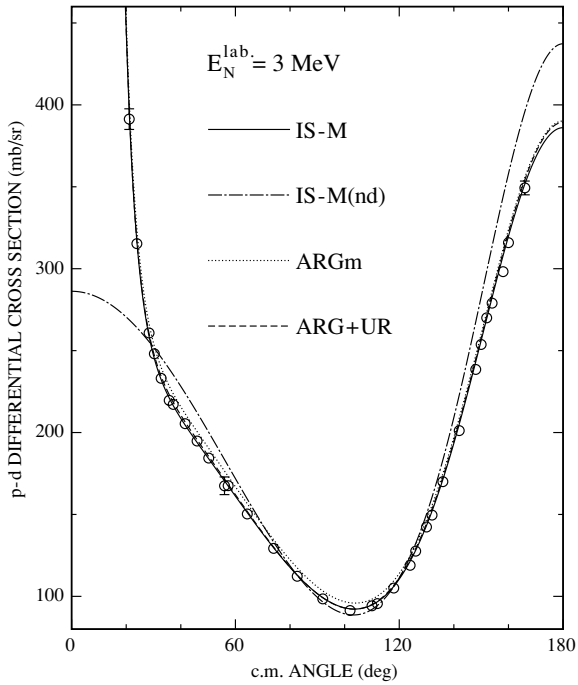

FIG. 5. *p-d* differential cross sections at a laboratory energy of 3 MeV. The experimental points are the measurement of Kocher and Clegg [16].

data are small. It seems that with the present models (local, local + 3N [9], and nonlocal forces) the best description of the minimum of T_{22} is given by the nonlocal IS-M set of interactions.

IV. SUMMARY AND CONCLUSIONS

The *n-d* calculations are much simpler than the *p-d* ones; however, the *p-d* measurements are more accurate, and more observables, such as tensor-analyzing powers, are available.

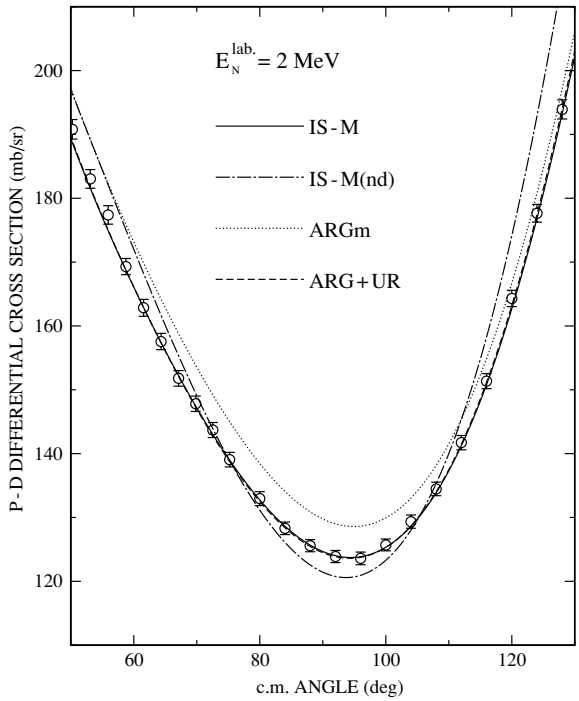

FIG. 4. The same as in Fig. 3 around the minimum region.

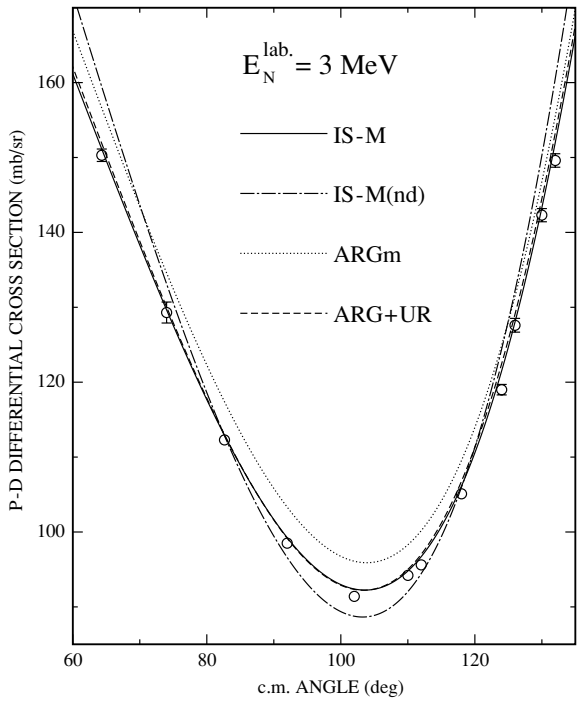

FIG. 6. The same as in Fig. 5 around the minimum region.

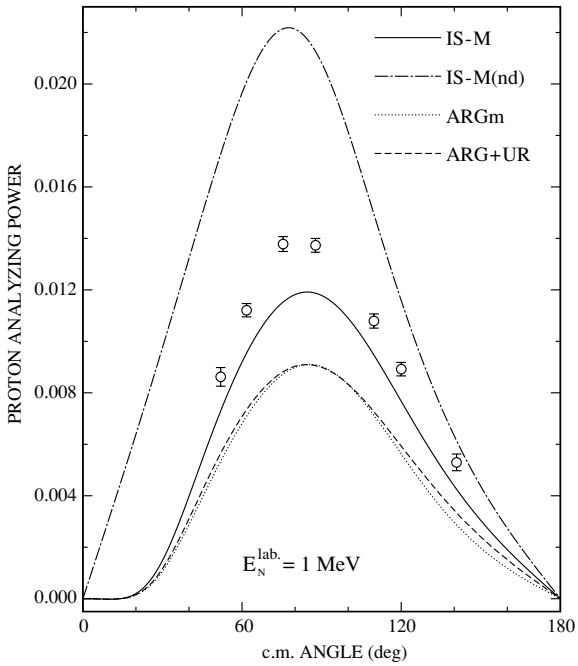

FIG. 7. The proton analyzing power of the *p-d* elastic scattering at a laboratory energy of 1 MeV. The experimental points are the measurement of Wood *et al*. [20].

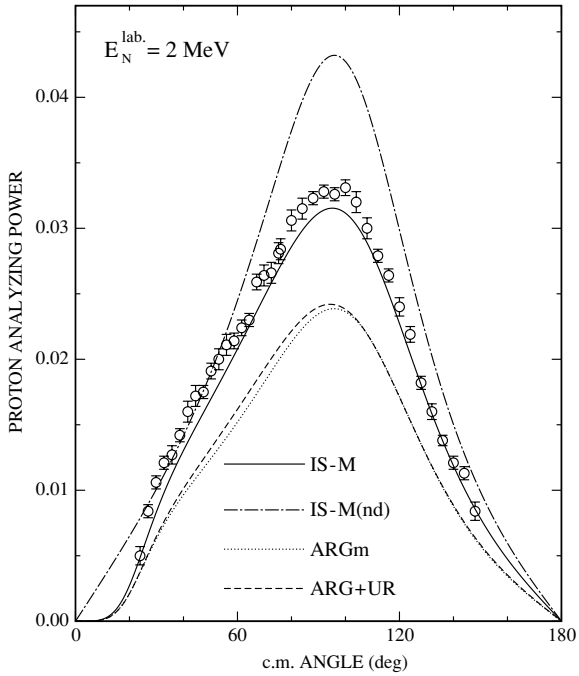

FIG. 9. The proton analyzing power of the *p-d* elastic scattering at a laboratory energy of 2 MeV. The experimental points are the measurement of Shimizu *et al*. [15].

Therefore, for a detailed investigation one has to study the *p-d* scattering. The inclusion of the Coulomb interaction in three-body calculations is a difficult and time-consuming task, and, to achieve a reasonable accuracy, we had to take a larger Coulomb-Sturmian basis (30–40 functions in each variable). This relatively large basis and the available computer resources (we used PCs) limits the number of included partial-wave components of the NN interaction to $j_{\max} = 4$, which, fortunately, was enough below the breakup threshold.

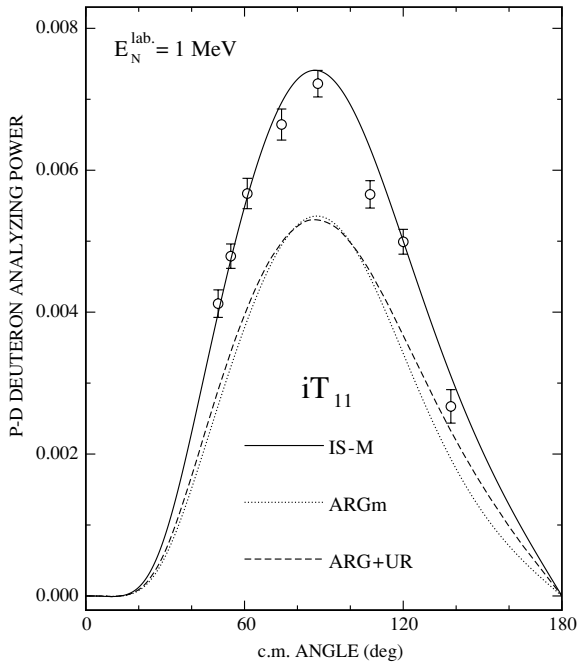

FIG. 8. The deuteron vector analyzing power iT_{11} of the *p-d* elastic scattering at a laboratory energy of 1 MeV. The experimental points are the measurement of Wood *et al*. [20].

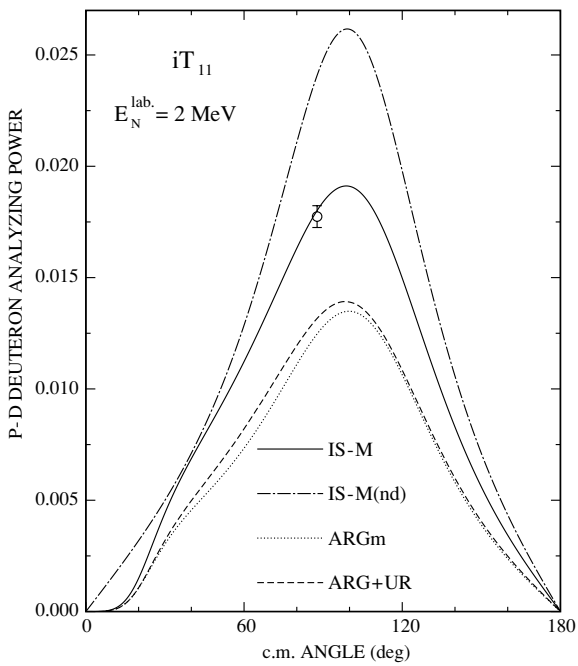

FIG. 10. The deuteron vector analyzing power iT_{11} of the *p-d* elastic scattering at a laboratory energy of 2 MeV. The experimental point is the measurement of Brune *et al*. [21].

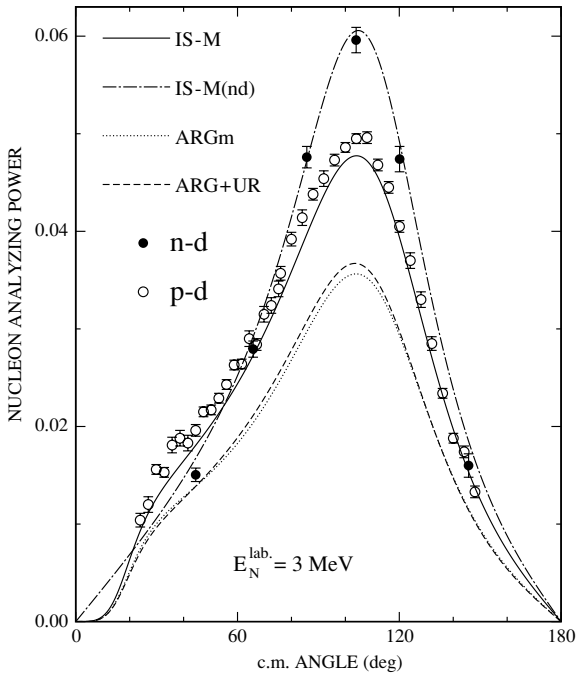

FIG. 11. The proton and neutron analyzing power of the *p-d* and *n-d* elastic scattering at a laboratory energy of 3 MeV. The experimental points are the measurement of Shimizu *et al*. [15].

The present results with the ARGm set of the interaction were compared to the ones calculated by Kievsky [20,21] with the full Argonne v_{18} interaction. There are some differences in the vector-analyzing power results. At 1 MeV the present results are larger, whereas at 3 MeV they are slightly smaller.

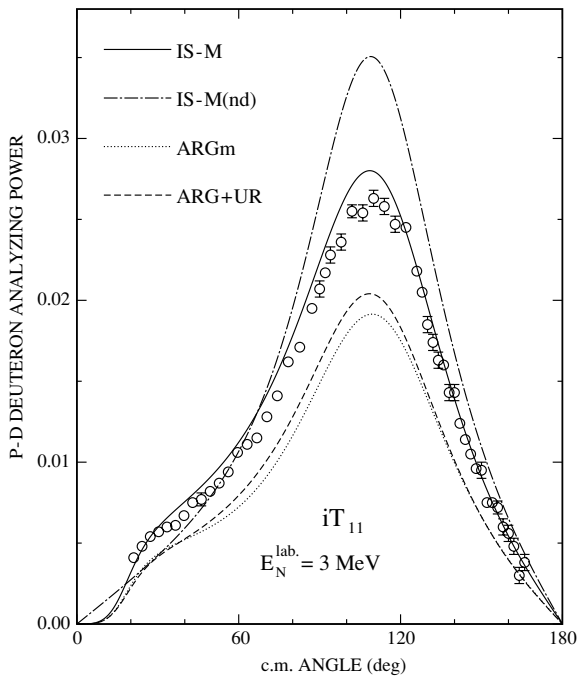

FIG. 12. The deuteron vector analyzing power iT_{11} of the *p-d* elastic scattering at a laboratory energy of 3 MeV. The experimental points are the measurement of Shimizu *et al*. [15].

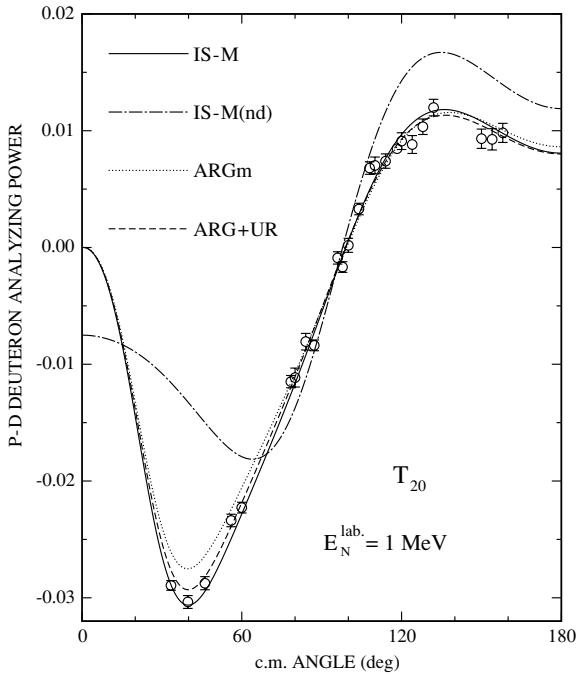

FIG. 13. The deuteron tensor analyzing power T_{20} of the *p-d* elastic scattering at a laboratory energy of 1 MeV. The experimental points are the measurement of Wood *et al*. [20].

However, the tensor-analyzing powers are very near to each other.

Because of the scaling law [17], it may be possible to reproduce the experimental *n-d* observables below the breakup threshold theoretically only if the model provides the correct ^3H and ^{3}He binding energies. This is especially true below the

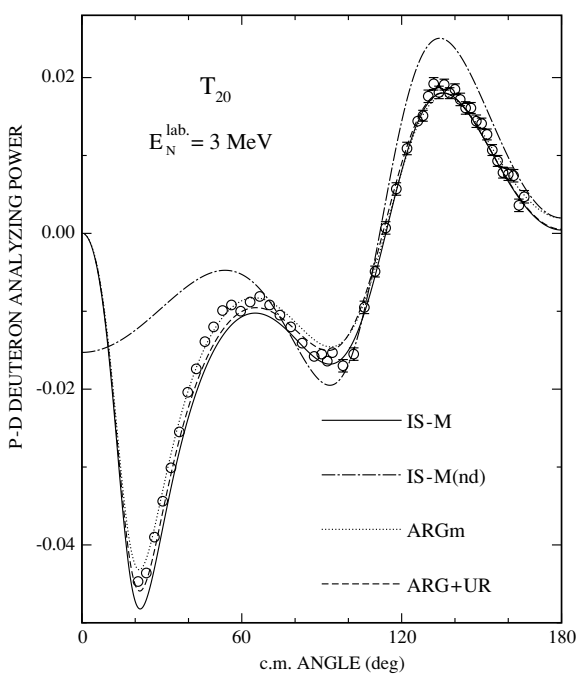

FIG. 14. The deuteron tensor analyzing power T_{20} of the *p-d* elastic scattering at a laboratory energy of 3 MeV. The experimental points are the measurement of Sagara [15].

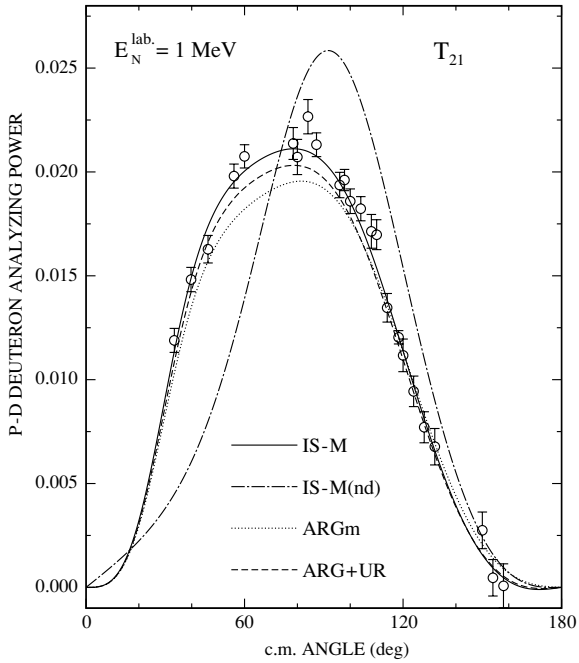

FIG. 15. The deuteron tensor analyzing power T_{21} of the *p-d* elastic scattering at a laboratory energy of 1 MeV. The experimental points are the measurement of Wood *et al*. [20].

breakup threshold, where the difference between the scattering energies and the the bound-state energy is small. Therefore, one cannot really expect a good description of the scattering data with the present local NN potentials, because none of them reproduces the 3N binding energies. Consequently, only

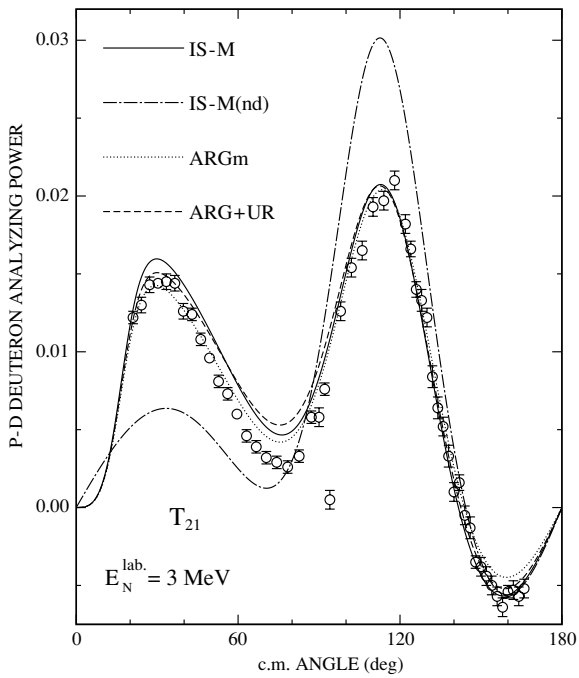

FIG. 16. The deuteron tensor analyzing power T_{21} of the *p-d* elastic scattering at a laboratory energy of 3 MeV. The experimental points are the measurement of Sagara [15].

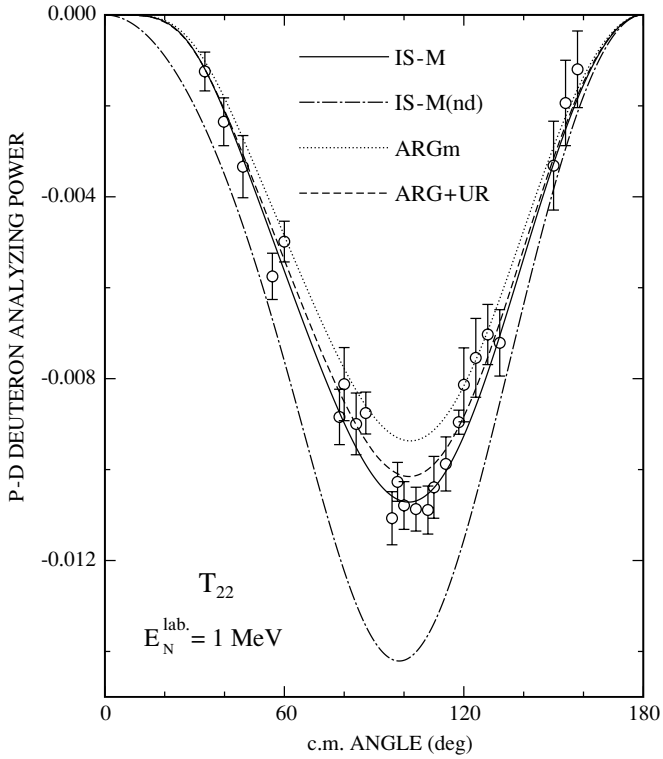

FIG. 17. The deuteron tensor-analyzing power T_{22} of the *p-d* elastic scattering at a laboratory energy of 1 MeV. The experimental points are the measurement of Wood *et al*. [20].

the local+3N and the nonlocal NN potential models could be compared.

To make this more transparent, the *p-d* results of Kievsky and collaborators [14,20,21,22] with the Argonne v_{18} plus Urbana 3N force (ARG+UR) are also shown in the figures.

The scaling effect is well demonstrated by the minima of the differential cross sections (Figs. 2, 4, and 6). It is clear that only the IS-M and ARG+UR interactions produce the correct minima. These interactions also produce excellent agreement with the measurements in the full angle range for all three energies.

The vector-analyzing powers are also improved with the IS-M set of interactions. This, however, is because of the modified triplet *P*-wave interactions, as was shown for the *n-d* scattering in Ref. [2] (IS-A versus IS-M). One does not expect any change of this effect by the Coulomb interaction. Also, the introduction of the 3N forces, the Urbana force in this case, does not produce any significant change.

The calculated proton analyzing powers with the IS-M interaction are close to the experimental values at 2 and 3 MeV (Figs. 9 and 11), but they seems to be much below at 1 MeV. There the *p-d* maximum is nearly half of the *n-d* one (Fig. 7), whereas at higher energies the Coulomb effect, as expected, is smaller. The electromagnetic forces do not seem to be strong enough to make up the difference [23].

However, if the energy dependence of the maximum of the measured *p-d* analyzing powers is plotted and compared with the *p-d* calculations of the IS-M set (Fig. 19), it becomes visible that the difference between the measured and calculated

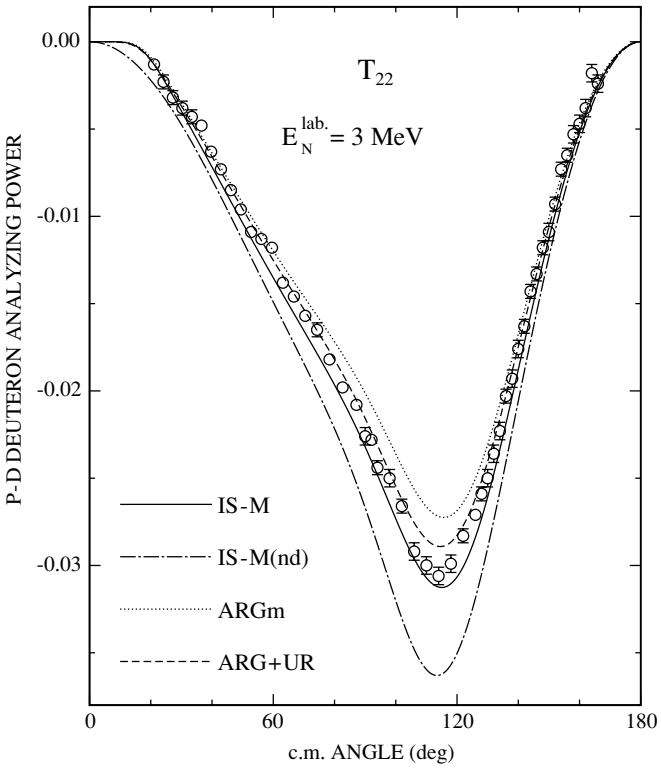

FIG. 18. The deuteron tensor-analyzing power T_{22} of the *p-d* elastic scattering at a laboratory energy of 3 MeV. The experimental points are the measurement of Sagara [15].

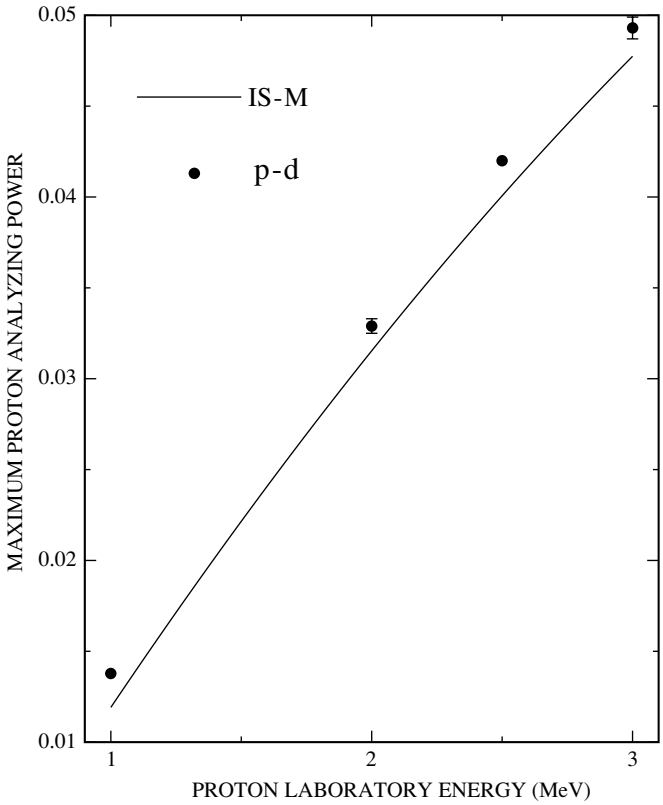

FIG. 19. The maximum of the measured and calculated *p-d* vector analyzing powers.

maximum values is approximately a constant. This difference produces a larger effect when the analyzing power is small.

The calculated deuteron vector analyzing powers with the IS-M interaction are in reasonable agreement with the measured ones at all three energies (Figs. 8, 10, and 12), although, at 2 MeV there is only one experimental point [22].

The *p-d* tensor-analyzing powers are measured only at 1 and 3 MeV [15,20]. At 1 MeV the IS-M seems to provide a better agreement with the measurements [20] than the ARGm and ARG+UR potentials (Figs. 13, 15, and 17) for all the three tensor-analyzing powers, although the error bars for experimental values are rather large. At 3 MeV all three *p-d* calculations (IS-M, ARGm, and ARG+UR) for T_{20} (Fig. 14) slightly differ from the experimental values. The T_{21} (Fig. 16) produces the same problem what was observed at higher energies (5 and 9 MeV in Ref. [2]). The forward angle T_{21} up to 80° is not reproduced by the theory, whereas above 100° the Coulomb effect produces an agreement with the experiments.

The T_{22} (Fig. 18) is worth for a closer look. In an earlier work, Ref. [2], it was predicted that the Coulomb shift would bring the minimum around 120°−130°, very close to the that experimental data. This would be important, because the T_{22} in the low-energy region is sensitive to the A_D/A_S normalization constant of the deuteron bound-state wave function [24,25]. One important property of the IS interaction is a lower value for the deuteron *D*-state probability and a higher value for A_D/A_S. The present calculated values of the T_{22} verify this expectations, the *p-d* calculations with the IS-M set of interactions reproduces the minimum of the T_{22}, whereas the calculations with ARGm or ARG+UR interactions fail to do this (Figs. 17 and 18). It has to be noted, however, that the 3N force (ARG+UR) produces an improvement in the above mentioned angle region which is probably because of the scaling effect. Another problem could be that if we consider the slopes of T_{22} at 3 MeV (below 100° and above the 130°) the situation is the opposite: the ARG+UR result seems to be better than those of the IS-M.

In summarizing the results of this investigation, one can conclude that the 3N calculations with IS-M set of interactions are definitely superior to the calculations with the Argonne v_{18} potential. For the vector-analyzing powers it is clearly the consequence of the modified triplet *P*-wave interaction. A similar improvment could be achieved if a similar change is made for the triplet *P*-wave interactions of the Argonne potential. However, in all the other cases, the effect of the wrong 3N binding energy, produced by the Argonne v_{18} potential, exists.

Comparing to the Argonne v_{18}+Urbana force, in most of the cases, the IS-M results are equivalent or better. Some of the differences are because of the modified triplet *P*-wave interactions. Certainly, a similar modification of the local potential in the local+3N force model would lead to a similar improvement. However, the tensor-analyzing power T_{22} seems to show some other effect. A possible spin-orbit 3N force may also change the vector analyzing powers [21]. However,

the tensor-analyzing power T_{22} at 3, 5, and 10 MeV seems not to be changed by this force. This can be a sign that the observed differences of the minimum of the T_{22}, calculated with the ARGm, ARG+UR, and IS-M sets (Figs. 17 and 18), are caused partly by the scaling and partly by the different deuteron properties. This effect seems to be present at higher energies too [2].

This indicates that the deuteron D-state probability and asymptotic normalization constant A_D/A_S may need to be revised. The new accurate measurements of the low-energy T_{22} (and some older ones at higher energies) could be a good tool for that. The present calculations indicate that a higher value than $A_D/A_S = 0.0250 - 0.0255$ is necessary to reproduce the backward minimum of T_{22}. The present value of $A_D/A_S = 0.02697$ of the IS interaction, which is in agreement with the values found by earlier analyses [24,26], seems to be a more suitable value than the presently accepted $0.00250 - 0.00255$ values. The problem is that the A_D/A_S value seems to be connected to the deuteron D-state probability [27], and therefore the local potentials are unable to produce a higher A_D/A_S value.

ACKNOWLEDGMENTS

The authors are thankful to A. Kievsky for providing the results of his calculations with the 3N force and the experimental results of Wood *et al.*, Brune *et al.*, and Shimizu and Sagara. This work received partial support from the grants OTKA T034334, OTKA T046791, OMAA 49öu16, NSF Phy-0243740, and from the Cottrell Research Corporation.

[1] P. Doleschall, I. Borbély, Z. Papp, and W. Plessas, Phys. Rev. C **67**, 064005 (2003).
[2] P. Doleschall, Phys. Rev. C **69**, 054001 (2004).
[3] P. Doleschall, Nucl. Phys. **A602**, 60 (1996); P. Doleschall and I. Borbély, Few-Body Syst. **27**, 1 (1999).
[4] P. Doleschall, Few-Body Syst. **23**, 149 (1998).
[5] J. Siemens and A. P. Vischer, Ann. Phys. (NY) **238**, 167 (1995).
[6] N. Auerbach, J. Hüfner, A. K. Kerman, and C. M. Shakin, Rev. Mod. Phys. **44**, 48 (1972).
[7] R. B. Wiringa, V. G. J. Stoks, and R. Schiavilla, Phys. Rev. C **51**, 38 (1995).
[8] T. Tornow and W. Tornow, Few-Body Syst. **26**, 1 (1999).
[9] A. Kievsky, M. Viviani, and S. Rosati, Phys. Rev. C **64**, 024002 (2001).
[10] Z. Papp, Phys. Rev. C **55**, 1080 (1997); Z. Papp, C.-Y. Hu, Z. T. Hlousek, B. Kónya, and S. L. Yakovlev, *ibid.* **63**, 062721 (2001).
[11] Gy. Bencze, P. Doleschall, C. Chandler, A. G. Gibson, and D. Walliser, Phys. Rev. C **43**, 992 (1991).
[12] G. A. Baker Jr. and J. L. Gammel, editors, *The Padé Approximant in Theoretical Physics* (Academic Press, New York, 1970).
[13] C. R. Chen, J. L. Friar, and G. L. Payne, Few-Body Syst. **31**, 13 (2001).
[14] A. Kievsky, M. H. Wood, C. R. Brune, B. M. Fisher, H. J. Karwowski, D. S. Leonard, E. J. Ludwig, S. Rosati, and M. Viviani, Phys. Rev. C **63**, 024005 (2001).
[15] S. Shimizu, K. Sagara, H. Nakamura, K. Maeda, T. Miwa, N. Nishimori, S. Ueno, T. Nakashima, and S. Morinobu, Phys. Rev. C **52**, 1193 (1995).
[16] D. C. Kocher and T. B. Clegg, Nucl. Phys. **A132**, 455 (1969).
[17] T. Frederico, I. D. Goldman, and S. K. Adhikari, Phys. Rev. C **37**, 949 (1988).
[18] S. C. Pieper, Nucl. Phys. **A193**, 529 (1972); S. C. Pieper and K. L. Kowalski, Phys. Rev. C **5**, 306 (1972).
[19] P. Doleschall, Phys. Lett. **B40**, 443 (1972).
[20] M. H. Wood, C. R. Brune, B. M. Fisher, H. J. Karwowski, D. S. Leonard, E. J. Ludwig, A. Kievsky, S. Rosati, and M. Viviani, Phys. Rev. C **65**, 034002 (2002).
[21] A. Kievsky, Phys. Rev. C **60**, 034001 (1999).
[22] C. R. Brune, W. H. Geist, H. J. Karwowski, E. J. Ludwig, K. D. Veal, M. H. Wood, A. Kievsky, S. Rosati, and M. Viviani, Phys. Rev. C **63**, 044013 (2001).
[23] A. Kievsky, M. Viviani, and L. E. Marcucci, Phys. Rev. C **69**, 014002 (2004).
[24] I. Borbély, W. Grüebler, B. Vuaridel, and V. König, Nucl. Phys. **A503**, 349 (1989).
[25] N. L. Rodning, and L. D. Knutson, Phys. Rev. C **41**, 898 (1990).
[26] I. Borbély, W. Grüebler, P. Schmelzbach, and B. Jenny, Phys. Lett. **B109**, 262 (1982); Nucl. Phys. **A416**, 281c (1984); V. G. J. Stoks, P. C. Van Campen, W. Spit, and J. J. de Swart, Phys. Rev. Lett. **60**, 1932 (1988).
[27] P. Doleschall and I. Borbély, Phys. Rev. C **62**, 054004 (2000).